Combined fibre atrophy and decreased muscle regeneration capacity driven by mitochondrial DNA alterations underlie the development of sarcopenia

Sammy Kimoloi[1,2]*, Ayesha Sen[1], Stefan Guenther[3], Thomas Braun[3], Tobias Brügmann[4,5], Philipp Sasse[5], Rudolf J. Wiesner[1,6,7] (iD), David Pla-Martín[1]*† (iD) & Olivier R. Baris[1,8]† (iD)

[1]Institute of Vegetative Physiology, University of Cologne, Faculty of Medicine and University Clinics, Köln, Germany; [2]Department of Medical Laboratory Sciences, Masinde Muliro University of Science and Technology, Kakamega, Kenya; [3]Max Planck Institute for Heart and Lung Research, Bad Nauheim, Germany; [4]Institute for Cardiovascular Physiology, University Medical Center, Göttingen, Germany; [5]Institute of Physiology I, Medical Faculty, University of Bonn, Bonn, Germany; [6]Center for Molecular Medicine Cologne, University of Cologne, Köln, Germany; [7]Cologne Excellence Cluster on Cellular Stress Responses in Aging-associated Diseases (CECAD), University of Cologne, Köln, Germany; [8]Equipe MitoLab, UMR CNRS 6015, INSERM U1083, Institut MitoVasc, Université d'Angers, Angers, France

Abstract

Background Mitochondrial dysfunction caused by mitochondrial (mtDNA) deletions have been associated with skeletal muscle atrophy and myofibre loss. However, whether such defects occurring in myofibres cause sarcopenia is unclear. Also, the contribution of mtDNA alterations in muscle stem cells (MuSCs) to sarcopenia remains to be investigated.
Methods We expressed a dominant-negative variant of the mitochondrial helicase, which induces mtDNA alterations, specifically in differentiated myofibres (K320E^{skm} mice) and MuSCs (K320E^{msc} mice), respectively, and investigated their impact on muscle structure and function by immunohistochemistry, analysis of mtDNA and respiratory chain content, muscle transcriptome and functional tests.
Results K320E^{skm} mice at 24 months of age had higher levels of mtDNA deletions compared with controls in soleus (SOL, 0.07673% vs. 0.00015%, $P = 0.0167$), extensor digitorum longus (EDL, 0.0649 vs. 0.000925, $P = 0.0015$) and gastrocnemius (GAS, 0.09353 vs. 0.000425, $P = 0.0004$). K320E^{skm} mice revealed a progressive increase in the proportion of cytochrome c oxidase deficient (COX$^-$) fibres in skeletal muscle cross sections, reaching a maximum of 3.03%, 4.36%, 13.58%, and 17.08% in EDL, SOL, tibialis anterior (TA) and GAS, respectively. However, mice did not show accelerated loss of muscle mass, muscle strength or physical performance. Histological analyses revealed ragged red fibres but also stimulated regeneration, indicating activation of MuSCs. RNAseq demonstrated enhanced expression of genes associated with protein synthesis, but also degradation, as well as muscle fibre differentiation and cell proliferation. In contrast, 7 days after destruction by cardiotoxin, regenerating TA of K320E^{msc} mice showed 30% of COX$^-$ fibres. Notably, regenerated muscle showed dystrophic changes, increased fibrosis (2.5% vs. 1.6%, $P = 0.0003$), increased abundance of fat cells (2.76% vs. 0.23%, $P = 0.0144$) and reduced muscle mass (regenerated TA: 40.0 mg vs. 60.2 mg, $P = 0.0171$). In contrast to muscles from K320E^{skm} mice, freshly isolated MuSCs from aged K320E^{msc} mice were completely devoid of mtDNA alterations. However, after passaging, mtDNA copy number as well as respiratory chain subunits and p62 levels gradually decreased.
Conclusions Taken together, accumulation of large-scale mtDNA alterations in myofibres alone is not sufficient to cause sarcopenia. Expression of K320E-Twinkle is tolerated in quiescent MuSCs, but progressively leads to mtDNA and respiratory chain depletion upon activation, *in vivo* and *in vitro*, possibly caused by an increased mitochondrial removal. Altogether, our results suggest that the accumulation of mtDNA alterations in myofibres activates regeneration during aging, which leads to sarcopenia if such alterations have expanded in MuSCs as well.

Keywords mtDNA deletions; Mutations; Myofibres; Muscle stem cells; Satellite cells; Mitochondria

Introduction

Mitochondria are dynamic organelles with various cellular functions, including ATP production, calcium handling and signalling, but also amino acid and lipid metabolism,[1] all critical for skeletal muscle function. Consequently, ageing-related mitochondrial dysfunction has long been suspected to play a role in sarcopenia.[2,3] One important factor driving mitochondrial dysfunction is the accumulation of large-scale mitochondrial DNA (mtDNA) rearrangements in muscle fibres.[4] These alterations (deletions and duplications/insertions) arise and accumulate progressively, probably due to errors during replication and/or inefficient repair of double-strand breaks, potentially caused by reactive oxygen species.[5] When exceeding a detrimental threshold, usually >60% of the total mtDNA pool, they cause fibre segments with severe respiratory chain (RC) defects, detectable histochemically as a decrease in the enzymatic activity of the cytochrome C oxidase complex (COX$^-$) and a compensatory increase in the activity of succinate dehydrogenase (SDH^{++}) (COX$^-$/SDH^{++}, ragged red fibres), which do not contain mtDNA-encoded subunits. These RC defects occur concomitantly to atrophy, splitting, breakage and loss of muscle fibres.[3,6]

Considering that only short longitudinal segments of a few (<5%) myofibres are affected by mtDNA alterations in most mammalian species at old age,[7,8] it remains unclear whether these defects and the subsequent RC deficiency are sufficient to cause sarcopenia, that is, loss of mass, strength and performance of the whole muscle. Moreover, damage or loss of myofibres activates efficient regeneration by resident muscle stem cells (MuSCs).[9] Therefore, myofibres damaged due to mtDNA alterations may be effectively repaired, unless the regenerative capacity of MuSCs is severely compromised as well. Importantly, previous evidence has already suggested that a decline in mitochondrial function is among the key cell intrinsic factors that impairs MuSC-dependent regeneration in aged muscles,[10] and indeed, depletion of these cells impaired adaptation to long-term physical exercise in mice.[11] Therefore, we investigated whether the accumulation of mtDNA alterations in myofibres of four different muscles (soleus, SOL; extensor digitorum longus, EDL; gastrocnemius, GAS; and tibialis anterior, TA) or in MuSCs, respectively, significantly contributes to sarcopenia.

Methods

Transgenic mice

K320E^{skm} mice (C57BL/6J) were generated by crossing MLC1f-Cre mice[12] with R26-K320E-Twinkle$^{loxP/+}$ mice.[13] K320E^{msc} mice were generated by expressing K320E-Twinkle under the control of MuSCs-specific Pax7-Cre^{ERT}.[14] Mice from both genders were included. All procedures were approved by the local authority (LANUV, approval number: 2013-A165 and 2019-A090).

Treadmill exercise performance and rotarod test

Physical performance of sedentary 12- and 20-month-old mice was evaluated by forced treadmill exercise. Mice received a total of three training sessions on two consecutive days followed by experimental measurements. To assess exercise performance, the initial speed of 5 cm/s was increased by 5 cm/s every 1 min for a total of 3 min and thereafter by 2 cm/s every 3 min until exhaustion. For motor balance and coordination, the initial constant speed of 4 rpm was accelerated to 20 rpm/min. The latency to fall on the first trial and the mean latency on the test day (fourth day) were analysed.

Ex vivo isometric force generation and fatigue measurements

All experiments were performed as described before.[15] Isometric force was measured by stimulating for 1.1 s (SOL) and 0.4 s (EDL) with long tetanic pulses every 3 min at increasing frequency (25–150 Hz). To measure fatigue, 0.35 s tetanic pulses of 100 Hz (SOL) or 125 Hz (EDL) were applied every 3.7 s, and the force decline during 10 min was normalized to baseline. The maximal specific tetanic force generated was determined from the plateau of force—frequency curves, and the specific force was calculated by dividing by the muscle cross-sectional area (wet weight (mg)/mean fibre length (mm) × 1.06 mg/mm^3 (estimated density)) as previously described.[16] The fatigue index was determined by dividing the forces at the respective time point by the force at the beginning of the long and short interval fatigue.

Regeneration experiments

For regeneration experiments, Pax7-Cre^{ERT} was activated by injecting mice intraperitoneally for 5 days with 75 mg/kg/day of tamoxifen (Merck). Two days after the last injection, mice were anaesthetized with 2% xylazine, 10% ketamine in 0.9% NaCl. Muscle regeneration was induced by injecting one TA with 50 μl of cardiotoxin (CTX) from *Naja mossambica* (Sigma). At specific time points, mice were sacrificed, and muscles were snap-frozen in

isopentane pre-cooled in liquid nitrogen and stored until needed.

Satellite cell isolation

Posterior hindlimb muscles were isolated from 6- to 8-week-old mice for *in vitro* proliferation analysis or at the indicated age for quiescent satellite cells analysis. In this case, K320E-Twinkle expression was induced at 3 months of age with tamoxifen as explained before. Muscles were isolated and digested with PBS containing 10 mg/mL Collagenase II, 4 mg/mL Dispase and 2.5 mM $CaCl_2$ for 1 h at 37°C. Satellite cells were isolated using a gentleMACS Dissociator, Satellite Cells Isolation Kit and a MACS separator following supplier's protocol (Miltenyi Biotec). For mtDNA analysis of aged mice, the pellet was directly used for DNA isolation. For proliferation experiments, cells were seeded on collagen-coated dishes in expansion medium (40% DMEM 4.5 g/L glucose containing Glutamax, 40% HAM's F10, 20% FBS, 2.5 ng/µL bFGF, 1× chick embryo extract and 1× penicillin/streptomycin). Expression of K320E-Twinkle was induced with 10 µM 4-hydroxytamoxifen (Sigma) for 48 h. Medium was replaced every second day, and cells were passaged before reaching confluency.

Statistics

All data were analysed with GraphPad Prism. Two-factor analysis of variance (ANOVA) was used to analyse data on age-dependent increase of mtDNA deletions, COX-deficient fibres and body weight. Spearman's correlation test was used to analyse the correlation between the proportions of COX-deficient fibres and centrally nucleated fibres. Statistical significance was accepted at $P < 0.05$. Data are reported as mean ± standard error of mean (SEM).

Results

K320E[skm] muscles show accelerated accumulation of mtDNA alterations and age-dependent COX deficiency

As shown in *Figure* 1A, multiple mtDNA alterations were detectable by long-range PCR in SOL of both genotypes at the age of 24 months. Using deep sequencing, we found recently that the majority of these species are duplications, that is, random insertions of mtDNA sequences leading to molecules larger than 16 kb.[17] However, K320E[skm] mice showed a much larger variety of such molecules and had significantly higher

levels of the representative 'mouse common deletions' 1, 3 and 17[18] (*Figure* S1) compared with controls in SOL (0.07673 vs. 0.00015, $P = 0.0167$), EDL (0.065 vs. 0.000925, $P = 0.0015$) and GAS (0.09353 vs. 0.000425, $P = 0.0004$; *Figure* 1B) when using qPCR. As an example, analysis of K320E[skm] GAS demonstrated that these selected deletions increased by a factor of 2.7 between the age of 12 and 24 months (*Figure* 1C). Sequential COX/SDH histochemistry revealed the presence of fibres with COX deficiency (COX⁻, blue) in K320E[skm] mice starting at 12 months and dramatically increasing between 18 and 24 months (*Figure* 1D–H). Importantly, the accumulation of COX⁻ fibres did not occur to the same extent in the different analysed muscles, ranging from 3% (EDL) to 17% (GAS) at 24 months (*Table* 1). mtDNA deletions have been shown to induce an increase in SDH activity due to a futile compensatory activation of mitochondrial biogenesis. Several COX⁻/SDH⁺⁺ fibres were apparent, particularly in GAS and TA but rarely in SOL and EDL of 24-month-old K320E[skm] mice (white asterisks in *Figure* 1D). Consistent with this, modified Gomori trichrome analysis revealed an increased number of ragged red fibres (RRF) in GAS, but not in SOL, of 24-month-old K320E[skm] mice (*Figure* S2A and S2B). Fibre-type analysis showed a marked shift in muscle normally rich in fast glycolytic Type IIb fibres (GAS) towards a higher proportion of Type I fibres (*Figure* S2C and S2D), but not in SOL (*Figure* S2C).

K320E[skm] mice show normal mass, physical performance and force generation of isolated muscles

Longitudinal sections showed atrophic regions in some COX⁻ fibres in K320E[skm] mice (*Figure* 2A) or even loss of muscle segments (*Figure* 2B, dashed lines), like in normally aged muscles of rat and humans.[5] However, the gross morphology of TA and of the entire triceps surae complex (TSC) and muscle mass of TA, EDL and SOL were not altered (*Figure* 2C and 2D). Moreover, the fibre number per area in GAS was similar at 12 and 24 months of age (*Figure* 2E). Collectively, these results indicated that the defects induced by mtDNA alterations in a small but relevant percentage of myofibres were not sufficient to cause accelerated loss of whole muscle mass.

To determine whether mitochondrial dysfunction impacts muscle strength independently of mass, we measured isometric force generation *ex vivo* in EDL and SOL isolated from 24-month-old mice. These muscles are enriched in Type IIb and Type I/IIa fibres, respectively. Both isometric twitch force and capacity to increase force following tetanic stimulation at increasing frequencies were similar between K320E[skm] and control mice (*Figure* 2F and 2G). There was also no difference in the rate of fatigue development (*Figure* 2H and
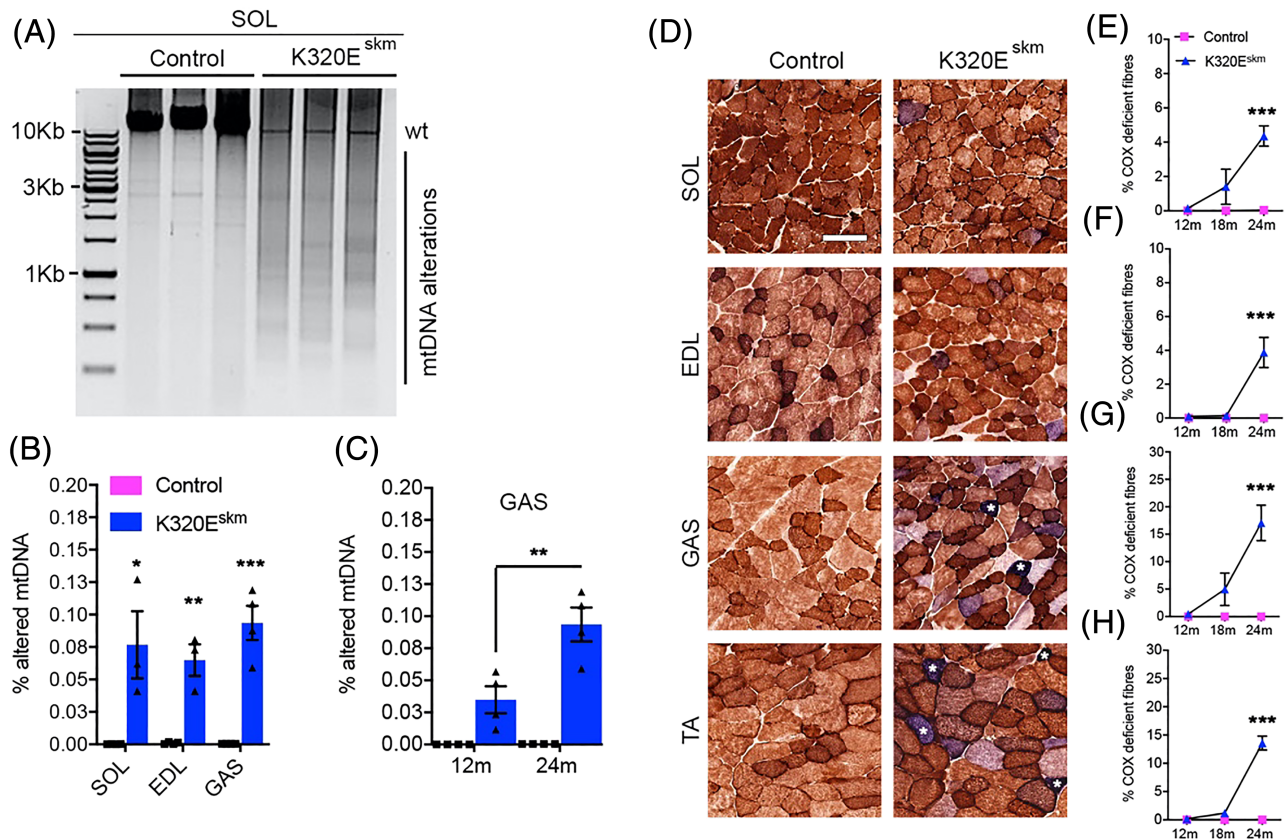
Figure 1 Expression of K320E-Twinkle in skeletal muscle accelerates the accumulation of mtDNA alterations and mitochondrial dysfunction. (A) Long-range PCR analysis showing multiple species of altered mtDNA in soleus (SOL) of 24-month-old K320E^{skm} mice. (B) qPCR analysis of three deletions (sum of Del 1, 3 and 17) in SOL, extensor digitorum longus (EDL) and gastrocnemius (GAS) muscles at 24 months of age. (C) qPCR analysis of K320E^{skm} GAS, showing ageing-dependent increase in deletion levels (sum of Del 1, 3 and 17). (D) Representative cross sections, showing COX-deficient (COX$^-$ and COX$^-$/SDH^{++} (white *) fibres in various hindlimb muscles at 24 months (TA, tibialis anterior). (E–H) COX-deficient fibre quantification showing accelerated and age-dependent increase of mitochondrial dysfunction. n = 3–6 mice/group were used for deletions analyses and n = 6–10 mice/group to quantify the proportion of COX$^-$ fibres. Data are expressed as mean ± SEM, ***P < 0.001. Scale bars, 100 µm.

Table 1 Cytochrome oxidase (COX) deficiency (%) in different hindlimb skeletal muscles

| Muscle | 12 months | | 18 months | | 24 months | | P value |
	Control	K320E-Twinkle^{skm}	Control	K320E-Twinkle^{skm}	Control	K320E-Twinkle^{skm}	
Soleus	0	0.15 ± 0.06	0	1.4 ± 1.02	0	4.36 ± 0.59	<0.0001
GAS	0	0.46 ± 0.25	0	5 ± 3	0	17.08 ± 3.23	<0.0001
TA	0	0.2 ± 0.07	0	1.18 ± 0.24	0	13.58 ± 1.22	<0.0001
EDL	0	0.12 ± 0.06	0	0.13 ± 0.05	0	3.03 ± 1.1	<0.0001

All values are mean ± SEM.

2I). Normalized cross-sectional areas (CSA) showed no difference for EDL and SOL between mutant and control mice (*Figure* S2E).

To investigate muscle function *in vivo*, we performed accelerating rotarod and forced treadmill exercise. As shown in *Figure* 2J, the latency to fall on the first trial and after 3 days of training (*Figure* 2K) was similar, both at 12 and 24 months of age. There was a significant drop in latency to fall at 24 months in both groups (*Figure* 2K), indicating that the exacerbated accumulation of mtDNA deletions in the mutants did not accelerate the normal ageing-dependent decline in motor coordination and balance. Running performance on a treadmill was also not impaired in K320E^{skm} mice. In fact, at 20 months of age, K320E^{skm} mice performed better than controls, as evidenced by a significantly higher total distance ran (*Figure*
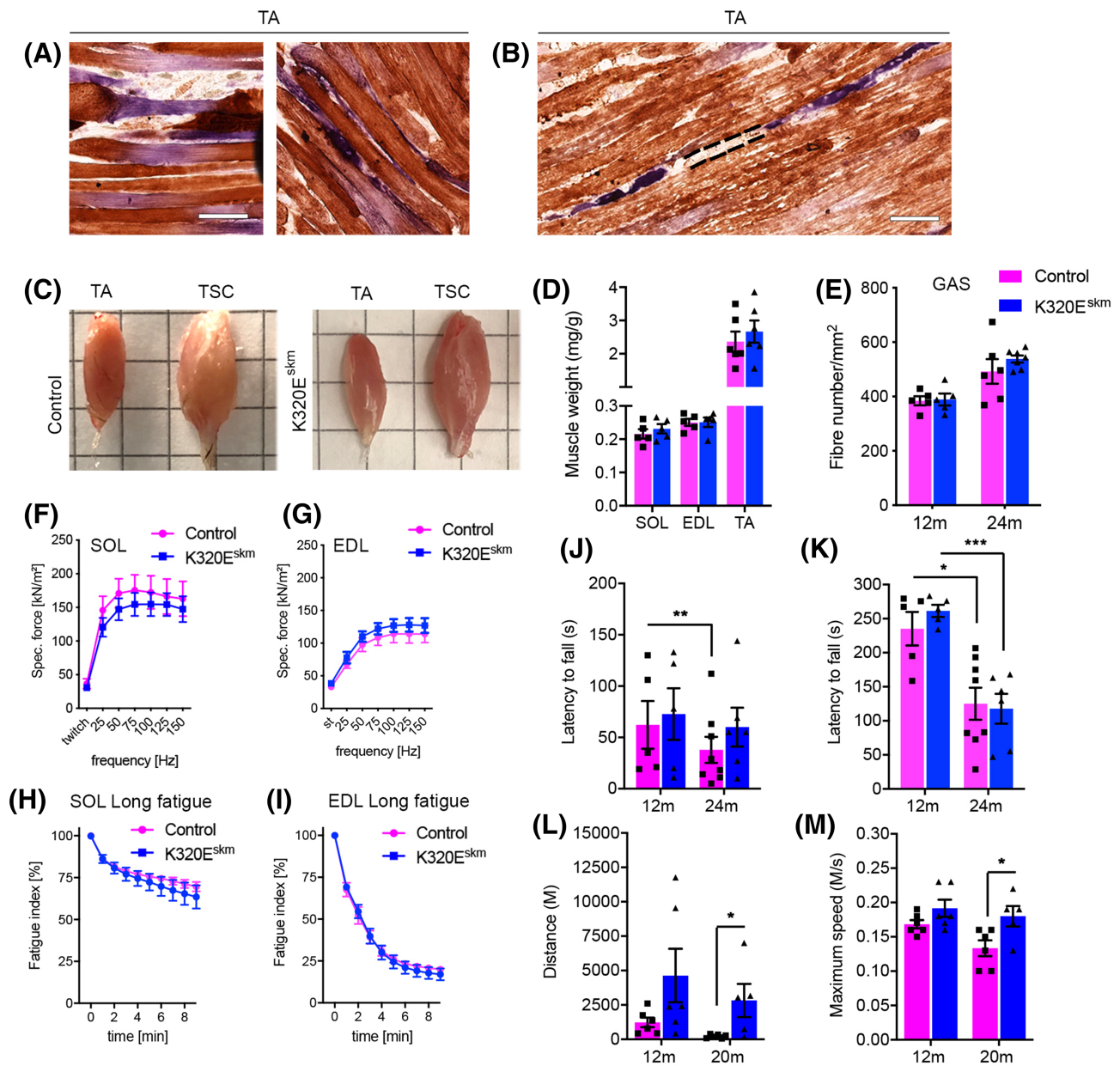
Figure 2 mtDNA alteration-induced defects in K320E-Twinkle[skm] do not affect muscle mass and function. (A) COX/SDH staining showing atrophic COX-[-/SDH++] fibres in TA muscle. (B) COX[-]/SDH[++] fibres with discontinuous segments in TA. (C) Gross morphology of TA and TSC (triceps surae complex). (D) Wet muscle weight normalized to body weight. (E) Fibre numbers per unit area in GAS. (F,G) *Ex vivo* specific twitch and tetanic force generation in SOL (F) and EDL (G). (H,I) Rate of fatigue development in SOL (H) and EDL (I) during 10 min of repetitive tetanic electrical stimulation *ex vivo.* The maximal specific tetanic force generated was determined from the plateau of the force–frequency curves. The fatigue index was determined by dividing the forces recorded at the beginning by the forces recorded at the end of the protocols. (J) Latency to fall on the very first rotarod trial and (K) after 3 days of training on rotarod. (L) Total distance run on treadmill and (M) maximum speed attained. Data are expressed as mean ± SEM; number of animals: rotarod test *n* = 5-6 mice/group, treadmill test *n* = 5–6 mice/group, *ex vivo* fatigue test *n* = 6–7 mice/group, *P* < 0.05, ***P* < 0.001. Scale bar 100 μm.

2L, *P* = 0.0321) and maximal speed attained (*Figure* 2M, *P* = 0.0408) on the treadmill. In summary, despite accumulating up to 17% of COX-deficient fibres in some muscles, whole muscle mass and motor performance were not compromised in K320E[skm] mice.

K320E[skm] *mice display signs of muscle regeneration but no signs of tissue deterioration*

Mice maintain robust skeletal muscle regeneration capacity even at 28 months of age.[19,20] We therefore hypothesized

that activation of MuSCs might have effectively counteracted loss of damaged fibres, thereby preventing loss of muscle mass and function even in old K320E^{skm} mice. Thus, we quantified newly generated fibres in GAS, identified as being central-nucleated, which carried the highest burden of COX$^-$ fibres. As shown in *Figure* 3A and 3B, there was a tendency towards an increased proportion of central-nucleated fibres (white asterisks) in K320E^{skm} muscles compared with controls (not significant, P = 0.094). However, consecutive sections stained for H&E or COX activity showed that all these central-nucleated fibres were COX positive (*Figure* 3C) and a strong positive correlation between the percentage of COX-deficient vs. the central-nucleated fibres (*Figure* 3D, r2 = 0.8, P = 0.006). Finally, Sirius Red and Oil Red O histochemical analyses did not reveal increased fibrosis and fat cell infiltration, respectively (*Figure* 3E–H). Collectively, these findings suggest that myofibre degeneration induced by mtDNA alterations in K320E^{skm} mice might have activated compensatory regeneration processes by resident muscle stem cells to maintain muscle mass and function.

Response to mtDNA alterations in skeletal muscle of K320E^{skm} mice

In order to characterize compensatory processes, we performed whole-exome RNA sequencing (RNAseq) in TA of 24-month-old mice, which carried a large burden of COX$^-$ fibres (*Figure* 1H). A total of 2287 genes were differentially expressed (adjusted P < 0.05; full list available at GEO database[21] (Accession number: GSE199201). Genes that showed differential expression between mutant and control mice with a fold change ≥ 1.5 are listed in *Table* S1 (upregulated genes) and *Table* S2 (downregulated genes). Upregulated genes included *methylenetetrahydrofolate dehydrogenase (NADP+ dependent) 2 (Mthfd2)*, *amine oxidase copper containing 1 (Aoc1)*, *sperm-associated antigen 5 (Spag5)*, *acyl-CoA thioesterase 2 (Acot2)*, and also *Peo1* encoding Twinkle, as expected from our genetic approach. The top downregulated genes include *monocyte to macrophage differentiation associated (Mmd)*, *phospholipase D family, member 5 (Pld5)*, *complement receptor type 2 (Cr2)*, and *adrenoceptor alpha 1A (Adra1a)*.

K320E expression in quiescent MuSCs leads to mtDNA depletion after activation

To test the hypothesis that efficient regeneration by MuSCs, which are not affected in K320E^{skm} mice, is responsible for alleviating the detrimental influence of mtDNA al-

terations in differentiated fibres, we designed a new conditional model in which expression of K320E-Twinkle is induced in satellite cells (Pax7Cre^{ERT}-mediated recombination, K320E^{msc} mice).

Expression of the transgene was induced by tamoxifen in 3-month-old mice, and MuSCs were isolated and immediately analysed at various ages (*Figure* 4A). In contrast to differentiated muscles, expression of the mutant helicase in quiescent MuSCs had not resulted in detectable mtDNA alterations, but had led to a significant decrease in mtDNA copy number at 18 months (*Figure* 4B). Next, K320E-Twinkle was induced *in vitro* in MuSCs isolated from 6- to 8-week-old mice (*Figure* 4C; GFP-positive cells). In freshly isolated, quiescent MuSCs (*Figure* 4D, Passage 0), the area of mitochondria per cell, assessed by TOM20 staining, was higher in K320E-Twinkle/Pax7 expressing cells (*Figure* 4E), which also showed increased expression of *Pgc1α* mRNA but unchanged expression of *Myod1* and *Myogenin* (*Figure* 4F), suggesting that compensatory mitochondrial biogenesis had occurred in the quiescent state *in vivo* without proliferation activation. In contrast, when isolated MuSCs were passaged (*Figure* 4G), proliferating cells expressing MYOD1 showed a decreased mitochondrial area (*Figure* 4H) and decreased mtDNA copy number (*Figure* 4I) at the last passage, despite sustaining high *Pgc1α* expression (*Figure* 4J). Accordingly, expression of index proteins of the respiratory chain complexes I, III and IV, as well as of the ATPase, all containing mtDNA encoded subunits, was decreased at passage 3 (*Figure* 4K and 4L). Moreover, at this passage, expression of the autophagy adaptor p62 was decreased by 50% in K320E MuSCs (*Figure* 4L), whereas LC3B-II levels were unchanged (*Figure* S3A and S3B). No mtDNA alterations could be detected in control and mutant cells at all investigated passages (data not shown). Last, after differentiation of MuSCs, despite lower levels of *Pgc1α*, mtDNA copy number was unchanged in K320E cells, suggesting that *in vitro*, differentiation is not affected (*Figure* S3C–S3E).

Altogether, our results indicate that expression of the mutant helicase is well tolerated in quiescent MuSCs, but progressively leads to mtDNA depletion when the cells are forced to proliferate in culture, possibly caused by an increased removal of mitochondria at later stages.

Muscle regeneration is impaired in K320E^{msc} mice in vivo and leads to a reduction of muscle mass and fibre type shift

Next, to activate MuSCs *in vivo*, muscle regeneration was triggered in K320E^{msc} mice by cardiotoxin injection. After 1 week of regeneration, mtDNA copy number was unchanged in mutant muscles (*Figure* 5A), but mtDNA alterations could be ob-
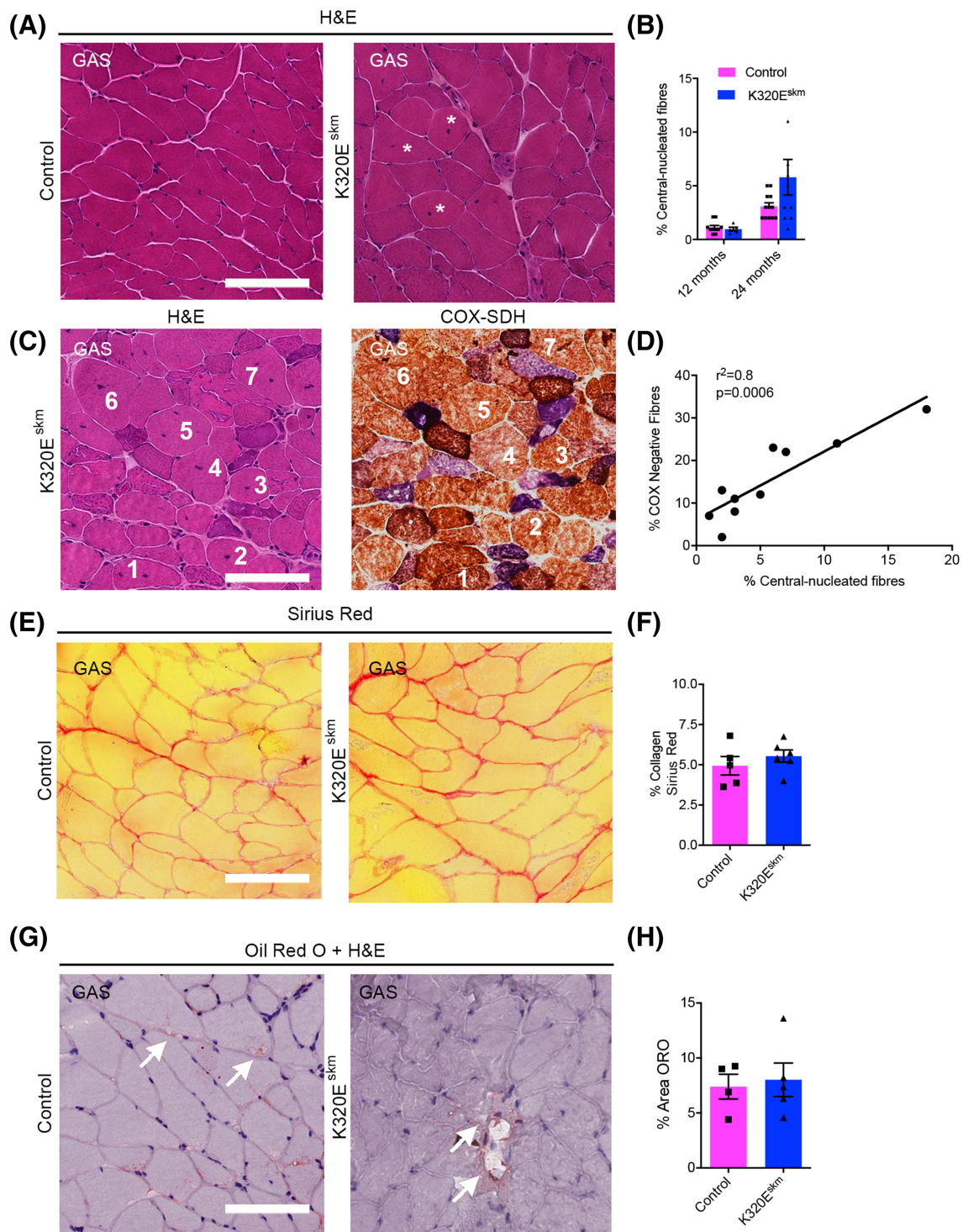
Figure 3 Histochemical analysis for regeneration, fibrosis and fat infiltration in gastrocnemius muscle. (A) Representative H&E pictures showing general tissue structure in GAS of 24-month-old mice, white asterisks depict fibres with central nuclei. (B) Percentage of central-nucleated fibres (12 months; n = 5 mice/per group, 24 months; n = 10–12 mice/group). (C) Serial sections stained with H&E and for COX-SDH showing COX-competent, regenerated (central nuclei) fibres (numbers depict same fibres) and (D) positive correlation between COX deficiency and percentage of central-nucleated fibres at 24 months. (E) Sirius red staining of GAS and (F) quantification of tissue occupied by collagen fibres. Fibrosis was estimated as the percentage of the relative area positive for Sirius Red staining in photomicrograph fields of 500 × 500 μm.(G) Fat deposition or adipocyte infiltration in GAS of 24-month-old mice and (H) quantification of Oil Red O (ORO) area. Data are expressed as mean ± SEM, n = 5 mice/group. Scale bar, 100 μm.
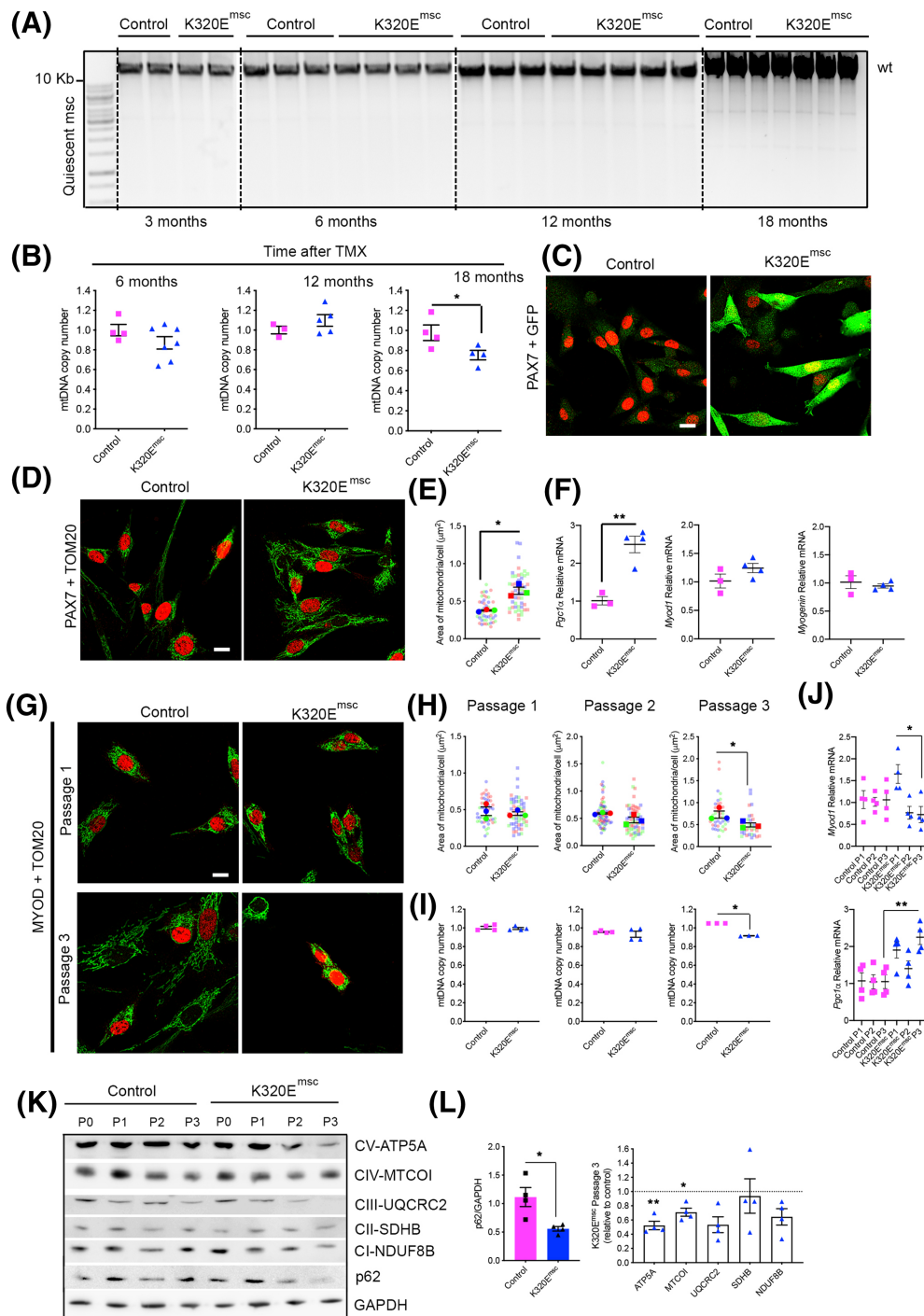
Figure 4 K320E-Twinkle expression in MuSCs leads to mtDNA depletion and increased autophagy. (A) Long-range PCR for mtDNA alterations and (B) mtDNA copy number quantification in MuSCs isolated at different time points after *in vivo* tamoxifen (TMX) induction (*n* = 3–6 mice per time point). (C, D) Representative confocal images of freshly isolated satellite cells from 6- to 8-week-old mice after 48-h 4-hydroxytamoxifen induction. α-GFP was used to monitor K320E-Twinkle expression, α-PAX7 as a satellite cell marker and α-TOM20 as a mitochondrial marker. (E) Quantification of the area occupied by mitochondria in PAX7+ cells. (F) Expression of *Pgc1α*, *Myod1* and *Myogenin* in freshly isolated satellite cells from 6- to 8-week-old mice after 48 h hydroxytamoxifen induction. (G) Confocal images of proliferative satellite cells at the indicated time points. α-MYOD was used as a MuSC proliferation marker. (H) Quantification of the area occupied by mitochondria in MYOD+ cells. (I) mtDNA copy number analysis in MuSCs at the indicated passage. (J) Expression of *Pgc1α* and *Myod1* in MuSCs at the indicated passage. (K,L) Western blot analysis and relative quantification of respiratory chain proteins and p62 after three passages in MuSCs total protein extracts (P, passage). GAPDH was used as a loading control. N = 4 mice. Data is expressed as mean ± SEM. For image analysis *n* = 3 mice, >15 cells per mouse. *P < 0.05. Scale bar, 10 μm.
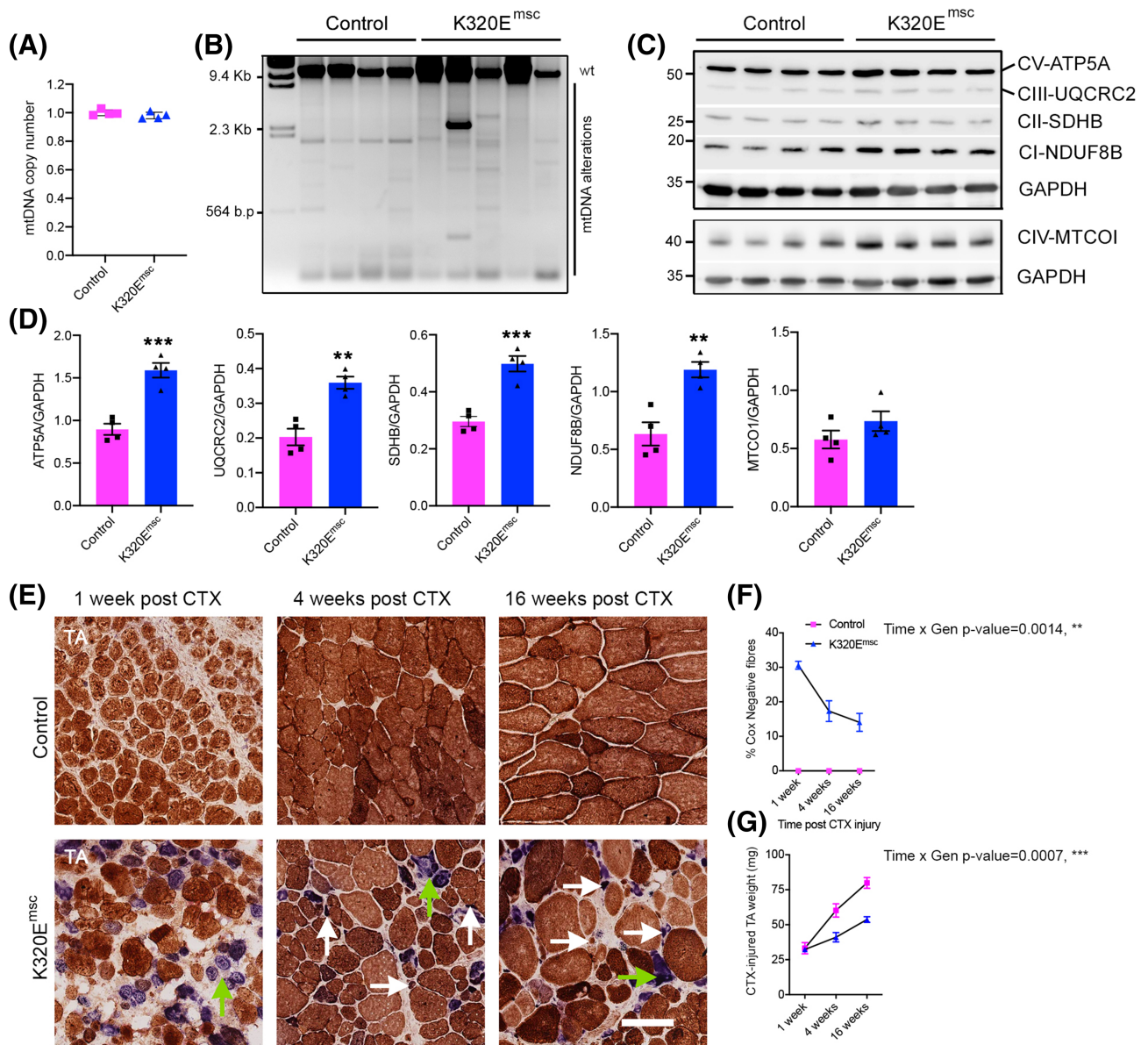
Figure 5 K320E-Twinkle expression in MuSCs causes mtDNA alterations and COX⁻ fibres upon regeneration. (A) mtDNA copy number analysis and (B) long-range PCR for mtDNA deletion screening in regenerated muscles from control and K320E^msc mice. (C,D) Western blot analysis and quantification of respiratory chain proteins in 7 days regenerated TA. GAPDH was used as a loading control. (E) Representative cross sections of regenerated TA muscles at the indicated time points stained for COX/SDH activity. COX-deficient fibre grouping is depicted by green arrows; white arrows depict atrophic fibres. (F) Quantitative analysis showing time-dependent decrease of COX-deficient fibres in regenerated K320E-Twinkle^msc TA muscle. (G) Analysis of absolute weights of the regenerated TA muscles in control and mutants. Data are expressed as mean ± SEM. **$P < 0.01$; ***$P < 0.001$. Scale bar, 100 μm.

served (*Figure* 5B), in striking contrast to induced, but quiescent MuSCs, even after 18 months (*Figure* 4A). Remarkably, index subunits of the respiratory chain complexes were increased in regenerated mutant muscles (*Figure* 5C and 5D), containing a striking accumulation of often clustered COX⁻ fibres, up to 30% at 7 days of regeneration (*Figure* 5E) and gradually decreasing to 15% at 16 weeks (*Figure* 5F). However, muscle mass remained 30% lower compared with the regenerated muscle of control mice (*Figure* 5G). Interestingly, a similar

15% of COX⁻ fibres was observed in K320E^skm mice at 24 months, which however showed no loss of muscle mass with ageing (*Figure* 1H). As expected, fibre type composition remained unchanged in non-injured muscles of both genotypes (*Figure* 6A and 6B). In contrast, after 1 month of regeneration, K320E^msc mice showed a fibre type shift with an increased proportion of fibre types I and IIA and a decreased proportion of glycolytic fibres of Type IIB (*Figure* 6A and 6C and *Figure* S3F). Fibre Types I and IIA are characterized by a
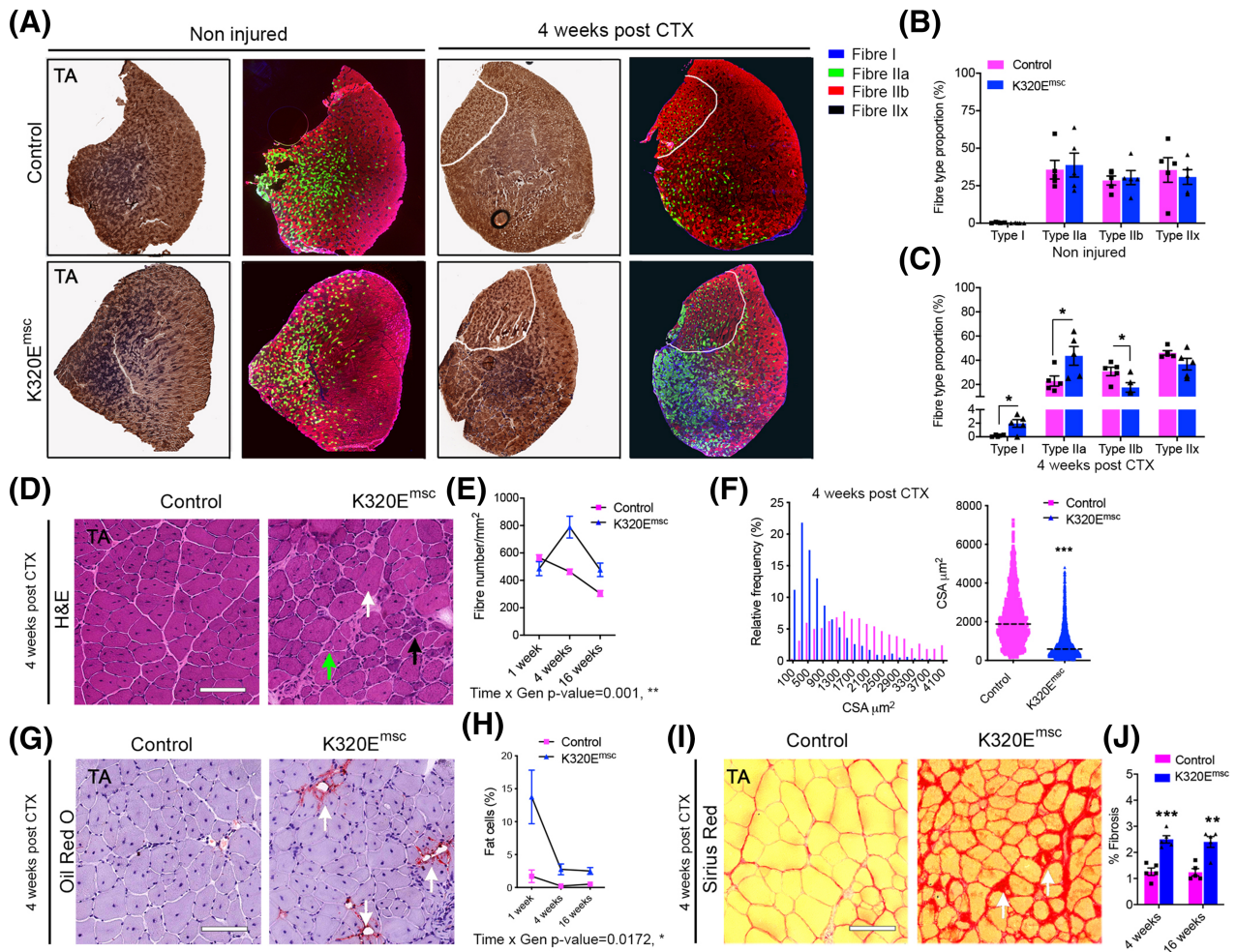
Figure 6 Mitochondrial DNA alterations in MuSCs impairs regeneration. (A) Representative cross sections of control and regenerated TA muscles stained for COX/SDH activity and for fibre types. α-MyHC-I, α-MyHC-2A and α-MyHC-2B were used a marker for Type I, Type IIa and Type IIb fibres. Fibre Type IIx was determined by negative staining. (B) Fibre type composition of the contralateral non-injured TA muscles and (C) 4 weeks post CTX injury. (D) Representative H&E pictures of injured muscle area in both mutant and control mice showing presence of regenerated fibres with central nuclei (white arrows), non-muscle cell infiltrates (black arrows) and severely atrophic fibres (green arrows). (E) Analysis of fibre number per unit injured areas. (F) Analysis of cross-sectional area distribution 4 weeks after regeneration. (G,H) Oil red O staining showing increased adipocyte infiltration in mutant mice at 4 weeks and quantitative analysis of fat cells in the injured TA muscles areas at 1, 4 and 16 weeks post injury. (I,J) Sirius red staining showing increased fibrosis at 4 weeks and quantitative analysis of fibrosis in the injured TA muscles areas at 4 and 16 weeks. Scale bar, 100 μm. Data are expressed as mean ± SEM. *$P < 0.05$; **$P < 0.01$; ***$P < 0.001$.

predominantly oxidative metabolism and a high mitochondrial content in mice, in line with the observed higher levels of respiratory chain subunits (*Figure* 5C and 5D). Quantitative analysis revealed a significant increase in fibre number over time (*Figure* 6D and 6E) and significantly decreased cross-sectional areas (*Figure* 6F) in mutant mice. Moreover, Oil Red O and Sirius Red staining showed increased fat cell infiltration (*Figure* 6G and 6H) and fibrosis (*Figure* 6I and 6J), respectively, in the regenerated muscle from K320E^msc mice compared with controls 4 and 16 weeks post regeneration. Last, inflammation was enhanced in regenerated mutant muscle after 1 week, as we observed increased infiltration of macrophages (*Figure* S4A and S4B), and basophils (*Figure* S4C and

S4D), as well as upregulation of *Il6* and *Ifn*β mRNA (*Figure* S4E). Thus, expression of K320E-Twinkle in MuSCs induces mtDNA alterations only upon their activation, which consequently severely impairs their regenerative capacity, leading to changes in muscle architecture and decreased muscle mass.

Discussion

In muscle of humans, monkeys, rats and mice as well as in other organs such as liver, heart and brain, ageing leads to the accumulation of mtDNA mutations, mostly deletions

and gene duplications, and is considered to be a hallmark of the ageing process.[22,23] In long-lived species, but not in mice, muscle fibre segments devoid of COX activity have been observed in old animals and have been postulated to be an important factor leading to sarcopenia.[2,24] In order to accelerate the formation of mtDNA alterations and study their contribution to sarcopenia in mice, we expressed specifically in skeletal muscle the dominant negative mutation K320E of the mitochondrial helicase Twinkle, which leads to the severe SANDO syndrome where patients present mtDNA deletions and suffer from myopathy.[25]

Surprisingly, the regular ageing-related decline in physical performance also observed in old humans was not accelerated in K320E^{skm} mice, although up to 17% COX$^-$ fibres were observed in muscle cross sections, implying that almost every fibre suffers from severe mitochondrial dysfunction in some segments along its longitudinal axis. In contrast, patients carrying a similar burden of COX$^-$ fibres complain about exercise intolerance and rapid muscle fatigue. Because the Twinkle mutation is present in every cell in patients, unlike in our mouse model, our results suggest that these symptoms may result from a combination of systemic and muscle intrinsic defects.

Due to ongoing regeneration from MuSCs, we also did not observe hallmarks of sarcopenia in K320E^{skm} mice, such as loss of muscle mass, fat infiltration or fibrosis. Consistent with enhanced presence of centrally nucleated fibres (*Figure* 3B), we found upregulation of the *Myh8* (+1.41-fold, *P* = 0.005784) and *Myh3* (+1.37-fold, *P* = 0.024631) genes in K320E^{skm} mice, which encode neonatal and embryonic myosin heavy chains, respectively. These isoforms are expressed early and transiently during muscle regeneration in adult mammals.[26] Moreover, GO enrichment analysis of all the differentially expressed genes also demonstrated significant enrichment of genes associated with cell proliferation processes (*Figure* S5, Panel B).

One major response to mtDNA alterations that recently emerged in the 'deletor mouse' model, which expresses a different mutant of Twinkle in the whole body,[27] is activation of an mTORC1-driven integrated stress response (ISR), leading to induction of *de novo* serine and mitochondrial tetrahydrofolate (mTHF) biosynthetic pathways and *de novo* nucleotide synthesis and asparagine synthetase.[28] As expected, these pathways are also activated in muscle of K320E^{skm} mice, indicated by induction of the genes encoding the *de novo* serine synthesis enzyme phosphoserine aminotransferase-1 (*Psat1*) as well as enzymes of the mTHF pathway (*Shmt2*, *Mthfd2*, and *Mthfd1l*) (*Table* S1). Increased activity of mTORC1 signalling promotes skeletal muscle protein synthesis,[29] and indeed, gene ontology (GO) enrichment analysis of all the 2287 differentially expressed genes showed that various terms associated with protein synthesis (translation, positive regulation of transcription, ribosome biogenesis and tRNA amino acylation) were over-represented among the signifi-

cantly enriched 'biological process' (BP) categories (*Figure* S5, Panel B). The terms ribosome and intracellular ribonucleoprotein were also among the top most five enriched 'cellular components' (CC) (*Figure* S5, Panel A), and terms associated with protein synthesis including structural constituent of ribosomes, poly(A) RNA binding and amino-acyl tRNA ligase activity were also among the most enriched 'molecular function' (MF) gene ontology terms (*Figure* S5, Panel C). Therefore, the persistent activation of mTORC1 in K320E^{skm} muscle is obviously important to maintain fibre size in the affected fibre segments. In agreement, treatment of 'deletor mice' with rapamycin, an mTORC1 inhibitor, alleviated most of the genetic and other alterations and reverted the progression of histological mitochondrial myopathy.[28]

However, in order to maintain normal muscle mass, protein synthesis and degradation processes have to be dynamically balanced. Notably, our RNAseq results also revealed significant upregulation of genes encoding key transcription factors that are known to promote muscle protein degradation including forkhead box-3 (*Foxo-3*; +1.37-fold, *P* = 0.001435), *Foxo-1* (+1.45-fold, *P* = 0.007729) and Kruppel-like factor 15 (Klf15; (1.23-fold, *P* = 0.019095). FOXO1 and FOXO3 promote autophagy and protein turnover mediated by the ubiquitin proteasomal system (UPS).[30–32] KLF15 is an upstream factor of glucocorticoids that drive muscle protein catabolism.[33] The muscle-specific ubiquitin ligase gene *Murf1*, genes encoding various subunits of the proteasome, lysosomal proton pumps and Calpains F and D were also upregulated in skeletal muscles of K320E^{skm} mice. Other differentially expressed genes are listed in *Tables* S1 and S2. Altogether, these results indicated induction of both anabolic and catabolic gene programs in the muscles of our K320E^{skm} model, leading to increased protein turnover in the constantly regenerating muscles.

Our data suggest that ongoing regeneration from the stem cell pool protects muscle from developing sarcopenia and contractile dysfunction, despite the high burden of mtDNA alterations and COX$^-$ segments. Therefore, we asked if accumulation of such mutations in MuSCs would impair regeneration. Surprisingly, expression of the mutant helicase in quiescent MuSCs had not resulted in detectable accumulation of mtDNA mutations over time *in vivo* (*Figure* 4A), not even 18 months after induction of its expression. Because K320E-Twinkle induces mtDNA alterations during the replication process, this either indicates an extremely slow mtDNA replication rate in the quiescent state of MuSCs or efficient mtDNA quality control mechanisms, much more efficient than those in differentiated muscle. However, 18 months after its induction, K320E-Twinkle expression led to a significant decrease in mtDNA copy number (*Figure* 4B), indicating either a slowing down of the mtDNA replication rate due to the slow unwinding activity of K320E-Twinkle or an exacerbated activation of quality control mechanisms (e.g. mitophagy), which are induced upon an increased mtDNA mutation load.[34]

Interestingly, freshly isolated K320E-MuSCs showed an increased mitochondrial area and upregulation of *Pgc1α*, indicating stimulation of mitochondrial biogenesis (*Figure* 4E), a response frequently observed following even mild mitochondrial dysfunction. In contrast, isolated MuSCs subjected to three passages to simulate activation (Figure 4G) showed a decreased mitochondrial mass (*Figure* 4H), decreased mtDNA copy number (*Figure* 4I) and consequently diminished respiratory chain subunit levels (*Figure* 4K and 4L) when expressing K320E-Twinkle. These data, together with decreased levels of the adapter protein p62 (*Figure* 4K and 4L) at the latest passage suggest an increased mitochondrial turnover, presumably activated to eliminate an excess of mtDNA damage. Consistently, no mtDNA alterations were found. Therefore, mtDNA alterations accumulate only in non-dividing and terminally differentiated cells. This phenomenon is also observed in patients suffering from mitochondrial disease, in which invasive and painful muscle biopsies are the gold standard for diagnosis because mtDNA mutations are not present in proliferative blood cells.[35] Besides regulating autophagy, p62 is essential to activate OXPHOS-induced selective mitophagy.[36] Because K320E- MuSCs suffer from a lack of mtDNA encoded OXPHOS subunits, the marked p62 downregulation, without changes in the autophagy marker LC3B-II, in proliferating cells might be reflecting a selective mechanism in charge of specific mitochondrial turnover. Hence, our results confirm that proliferating cell types—but most importantly also quiescent stem cells—have specific mechanisms to purify the mitochondrial pool from mutated mtDNA molecules. Nevertheless, further experiments to identify the molecular players of these mechanisms are needed.

Finally, induction of muscle regeneration showed that during the massive expansion of the mitochondrial pool, necessary when small quiescent MuSCs differentiate into large muscle fibres, mtDNA alterations accumulated in K320E^msc muscles and led to a marked accumulation of COX⁻ fibres, reaching proportions of up to 30% (*Figure* 5F). Many of the newly formed fibres disappear in the following recovery period, and, after 16 weeks, only 15% of COX⁻ fibres are left. Importantly, the regenerated muscle in K320E^msc mice does not regain the same mass compared with the contralateral, non-injured muscle or to those of control mice (*Figure* 5G). This is in part due to a fibre type shift from large, glycolytic Type IIb fibres to small-diameter oxidative IIa and Type I fibres (*Figure* 6C), also seen by increased respiratory chain subunit levels in regenerated muscle (*Figure* 5D). However, the lower mass is mainly due to atrophy and the partial loss of COX⁻ fibres, as demonstrated by a higher fibre number per unit area in K320E^msc mice and a decreased CSA (*Figure* 6E and 6F). The fibre type switch alone does not account for the loss of mass, because even if fibre types IIa and I are increasing in number, they are atrophic and smaller compared with the same types in control mice and even some COX-competent cells are smaller in size. In addition, fat infiltration and fibrosis occurs during regeneration, indicating mtDNA alterations as one of the intrinsic factors that impairs MuSCs-mediated regeneration (*Figure* 6G–J). Importantly, fibrosis and fat infiltration are also observed in human sarcopenia.[37,38] During its development, the loss of mass is mainly due to atrophy of large glycolytic Type IIx fibres and to a minor extent due to their preferential loss and a similar initial fibre type switch to Type I, which however are also lost later in humans.[39,40] Altogether, our results suggest that the accumulation of mtDNA alterations in myofibres activates regeneration during ageing, ultimately leading to sarcopenia if such alterations had been present at low levels in MuSCs as well and expanded during the regeneration process.

Conflict of interest

None declared.

Online supplementary material

Additional supporting information may be found online in the Supporting Information section at the end of the article.

References

1. Spinelli JB, Haigis MC. The multifaceted contributions of mitochondria to cellular metabolism. *Nat Cell Biol* 2018;**20**: 745–754.

2. Bua EA, McKiernan SH, Wanagat J, McKenzie D, Aiken JM. Mitochondrial abnormalities are more frequent in muscles undergoing sarcopenia. *J Appl Physiol (1985)* 2002;**92**:2617–2624.

3. Herbst A, Pak JW, McKenzie D, Bua E, Bassiouni M, Aiken JM. Accumulation of mitochondrial DNA deletion mutations in aged muscle fibers: Evidence for a causal role in muscle fiber loss. *J Gerontol A Biol Sci Med Sci* 2007;**62**:235–245.

4. Herbst A, Lee CC, Vandiver AR, Aiken JM, McKenzie D, Hoang A, et al. Mitochondrial DNA deletion mutations increase exponentially with age in human skeletal muscle. *Aging Clin Exp Res* 2021;**33**:1811–1820.

5. Bua E, Johnson J, Herbst A, Delong B, McKenzie D, Salamat S, et al. Mitochondrial DNA-deletion mutations accumulate intracellularly to detrimental levels in aged human skeletal muscle fibers. *Am J Hum Genet* 2006;**79**:469–480.

6. Wanagat J, Cao Z, Pathare P, Aiken JM. Mitochondrial DNA deletion mutations colocalize with segmental electron transport system abnormalities, muscle fiber atrophy, fiber splitting, and oxidative damage in sarcopenia. *FASEB J* 2001;**15**:322–332.

7. Brierley EJ, Johnson MA, Lightowlers RN, James OF, Turnbull DM. Role of mitochondrial DNA mutations in human aging: Implications for the central nervous system and muscle. *Ann Neurol* 1998;**43**:217–223.

8. McKiernan SH, Colman R, Lopez M, Beasley TM, Weindruch R, Aiken JM. Longitudinal analysis of early stage sarcopenia in aging rhesus monkeys. *Exp Gerontol* 2009;**44**: 170–176.

9. Wang YX, Rudnicki MA. Satellite cells, the engines of muscle repair. *Nat Rev Mol Cell Biol* 2011;**13**:127–133.

10. Zhang H, Ryu D, Wu Y, Gariani K, Wang X, Luan P, et al. NAD(+) repletion improves mitochondrial and stem cell function and enhances life span in mice. *Science* 2016; **352**:1436–1443.

11. Englund DA, Murach KA, Dungan CM, Figueiredo VC, Vechetti IJ Jr, Dupont-Versteegden EE, et al. Depletion of resident muscle stem cells negatively impacts running volume, physical function, and muscle fiber hypertrophy in response to lifelong physical activity. *Am J Physiol Cell Physiol* 2020;**318**:C1178–C1188.

12. Bothe GW, Haspel JA, Smith CL, Wiener HH, Burden SJ. Selective expression of Cre recombinase in skeletal muscle fibers. *Genesis* 2000;**26**:165–166.

13. Baris OR, Ederer S, Neuhaus JF, von Kleist-Retzow JC, Wunderlich CM, Pal M, et al. Mosaic deficiency in mitochondrial oxidative metabolism promotes cardiac arrhythmia during aging. *Cell Metab* 2015;**21**: 667–677.

14. Gunther S, Kim J, Kostin S, Lepper C, Fan CM, Braun T. Myf5-positive satellite cells contribute to Pax7-dependent long-term maintenance of adult muscle stem cells. *Cell Stem Cell* 2013;**13**:590–601.

15. Bruegmann T, van Bremen T, Vogt CC, Send T, Fleischmann BK, Sasse P. Optogenetic control of contractile function in skeletal muscle. *Nat Commun* 2015;**6**:7153.

16. Lynch GS, Hinkle RT, Chamberlain JS, Brooks SV, Faulkner JA. Force and power output of fast and slow skeletal muscles from mdx mice 6-28 months old. *J Physiol* 2001;**535**:591–600.

17. Basu S, Xie X, Uhler JP, Hedberg-Oldfors C, Milenkovic D, Baris OR, et al. Accurate mapping of mitochondrial DNA deletions and duplications using deep sequencing. *PLoS Genet* 2020;**16**:e1009242.

18. Oexner RR, Pla-Martín D, Paß T, Wiesen MHJ, Zentis P, Schauss A, et al. Extraocular muscle reveals selective vulnerability of type IIB fibers to respiratory chain defects induced by mitochondrial DNA alterations. *Invest Ophthalmol Vis Sci* 2020;**61**:14.

19. Lee AS, Anderson JE, Joya JE, Head SI, Pather N, Kee AJ, et al. Aged skeletal muscle retains the ability to fully regenerate functional architecture. *Bioarchitecture* 2013;**3**:25–37.

20. Shavlakadze T, McGeachie J, Grounds MD. Delayed but excellent myogenic stem cell response of regenerating geriatric skeletal muscles in mice. *Biogerontology* 2010;**11**: 363–376.

21. Barrett T, Wilhite SE, Ledoux P, Evangelista C, Kim IF, Tomashevsky M, et al. NCBI GEO: Archive for functional genomics data sets--Update. *Nucleic Acids Res* 2013;**41**: D991–D995.

22. Larsson NG. Somatic mitochondrial DNA mutations in mammalian aging. *Annu Rev Biochem* 2010;**79**:683–706.

23. Lopez-Otin C, Blasco MA, Partridge L, Serrano M, Kroemer G. The hallmarks of aging. *Cell* 2013;**153**:1194–1217.

24. Aiken J, Bua E, Cao Z, Lopez M, Wanagat J, McKenzie D, et al. Mitochondrial DNA dele-tion mutations and sarcopenia. *Ann N Y Acad Sci* 2002;**959**:412–423.

25. Hudson G, Deschauer M, Busse K, Zierz S, Chinnery PF. Sensory ataxic neuropathy due to a novel C10Orf2 mutation with probable germline mosaicism. *Neurology* 2005;**64**:371–373.

26. d'Albis A, Couteaux R, Janmot C, Roulet A, Mira JC. Regeneration after cardiotoxin injury of innervated and denervated slow and fast muscles of mammals. *Myosin isoform analysis European journal of biochemistry* 1988;**174**:103–110.

27. Tyynismaa H, Mjosund KP, Wanrooij S, Lappalainen I, Ylikallio E, Jalanko A, et al. Mutant mitochondrial helicase Twinkle causes multiple mtDNA deletions and a late-onset mitochondrial disease in mice. *Proc Natl Acad Sci USA* 2005;**102**: 17687–17692.

28. Khan NA, Nikkanen J, Yatsuga S, Jackson C, Wang LY, Pradhan S, et al. mTORC1 regulates mitochondrial integrated stress response and mitochondrial myopathy progression. *Cell Metab* 2017;**26**: 419–428.e5.

29. Egerman MA, Glass DJ. Signaling pathways controlling skeletal muscle mass. *Critical reviews in biochemistry and molecular biology* 2014;**49**:59–68.

30. Mammucari C, Milan G, Romanello V, Masiero E, Rudolf R, Del Piccolo P, et al. FoxO3 controls autophagy in skeletal muscle in vivo. *Cell Metab* 2007;**6**: 458–471.

31. Yamazaki Y, Kamei Y, Sugita S, Akaike F, Kanai S, Miura S, et al. The cathepsin L gene is a direct target of FOXO1 in skeletal muscle. *Biochem J* 2010;**427**: 171–178.

32. Zhao J, Brault JJ, Schild A, Cao P, Sandri M, Schiaffino S, et al. FoxO3 coordinately activates protein degradation by the autophagic/lysosomal and proteasomal pathways in atrophying muscle cells. *Cell Metab* 2007;**6**:472–483.

33. Shimizu N, Yoshikawa N, Ito N, Maruyama T, Suzuki Y, Takeda S, et al. Crosstalk between glucocorticoid receptor and nutritional sensor mTOR in skeletal muscle. *Cell Metab* 2011;**13**:170–182.

34. Garcia-Prat L, Martinez-Vicente M, Perdiguero E, Ortet L, Rodriguez-Ubreva J, Rebollo E, et al. Autophagy maintains stemness by preventing senescence. *Nature* 2016;**529**:37–42.

35. Ahmed ST, Craven L, Russell OM, Turnbull DM, Vincent AE. Diagnosis and

treatment of mitochondrial myopathies. *Neurotherapeutics* 2018;**15**:943–953.

36. Abudu YP, Shrestha BK, Zhang W, Palara A, Brenne HB, Larsen KB, et al. SAMM50 acts with p62 in piecemeal basal- and OXPHOS-induced mitophagy of SAM and MICOS components. *J Cell Biol* 2021;**220**.

37. Kent-Braun JA, Ng AV, Young K. Skeletal muscle contractile and noncontractile com- ponents in young and older women and men. *J Appl Physiol (1985)* 2000;**88**: 662–668.

38. Kirkeby S, Garbarsch C. Aging affects dif- ferent human muscles in various ways. An image analysis of the histomorphometric characteristics of fiber types in human masseter and vastus lateralis muscles from young adults and the very old. *Histol Histopathol* 2000;**15**: 61–71.

39. Lexell J. Human aging, muscle mass, and fiber type composition. *J Gerontol A Biol Sci Med Sci* 1995;**50**: Spec No:11-6. 50A 16.

40. Schiaffino S, Reggiani C. Fiber types in mammalian skeletal muscles. *Physiol Rev* 2011;**91**:1447–1531.